Biomedicine & Pharmacotherapy 79 (2016) 102–111

Available online at
ScienceDirect
www.sciencedirect.com

Elsevier Masson France
EM|consulte
www.em-consulte.com/en

Original article

Endostatin gene therapy inhibits intratumoral macrophage M2 polarization

Karen Foguer[a,b,*], Marina de Souza Braga[a,b], Jean Pierre Schatzmann Peron[c], Karina Ramalho Bortoluci[d], Maria Helena Bellini[a,b]

[a] Nephrology Division, Federal University of Sao Paulo, Sao Paulo, Brazil
[b] Biotechnology Department, IPEN-CNEN, Sao Paulo, Brazil
[c] Department of Immunology, Institute of Biomedical Sciences, University of São Paulo, São Paulo, Brazil
[d] Departament of Biology Biological Sciences, Federal University of Sao Paulo, Sao Paulo, Brazil

ARTICLE INFO

Article history:
Received 28 October 2015
Received in revised form 27 January 2016
Accepted 27 January 2016

Keywords:
Renal cell carcinoma
Endostatin
Tumor-associated macrophages

ABSTRACT

Background: Renal cell carcinoma (RCC) is a highly vascularized cancer resistant to chemotherapy and radiotherapy. RCC is frequently infiltrated with immune cells, with macrophages being the most abundant cell type. Alternatively activated M2 macrophages are known to contribute to tumor progression. Endostatin (ES) is a fragment of collagen XVIII that possesses antiangiogenic activity. In this study, we investigated the impact of ES gene therapy on the polarization of tumor-associated macrophages (TAMs) in lung metastases from tumor-bearing mice.
Methods: BALB/c mice divided into three groups: Normal, Control and ES-treated. Tumor-bearing mice were treated with ES-transduced cells or control cells over ten days. At the end of the study, plasma was collected, and pulmonary macrophages were isolated and used for FACS or RT-PCR. ELISA tests were used to analyze plasma and cell culture supernatant cytokines.
Results: ES treatment significantly reduced the levels of anti-inflammatory and pro-angiogenic cytokines, including IL4, IL-10, IL-13 and VEGF. Gene expression of M2 markers, such as IL-10, Arg-1, VEGF and YM-1, declined significantly. Flow cytometry showed a reduction in the number of M2 F4/80 + CD36 + CD206 + CD209+ macrophages and in IL-10 secretion by these cells. Reduced levels of IL-10 were also found in the culture supernatants of the ES-treated group.
Conclusions: Our research corroborates previous observations that ES has an important anti-tumoral role. However, aside from promoting interferon-γ secretion and an effective T cell response, we show here that this switch is extended to TAMs, complicating the maintenance of pro-tumorigenic M2 macrophages and thus favoring tumor elimination.

© 2016 Elsevier Masson SAS. All rights reserved.

1. Introduction

Macrophages are among the most important cells of the innate immune system due to their capacity to effectively stimulate adaptive immune responses and to promote tissue homeostasis and repair. In fact, macrophages are widely distributed throughout the whole body and are known as tissue-resident cells that have tissue-specific nomenclatures: Kupffer cells reside in the liver, microglial cells in the central nervous system, Langerhans cells in the skin, osteoclasts in the bones and many others. It is now accepted that many of these cells are first derived from the yolk sac, which may greatly differ from monocyte-derived inflammatory macrophages that are recruited to inflamed tissues (reviewed in [1,2]).

In addition to being defined by their tissue specificity, peritoneal [3] or bone marrow-derived macrophages may also be characterized by their phenotype, or more precisely, by their biological activities. In this sense, macrophages may differ greatly in function, and discrepant populations have been described [2,3]. Indeed, it is currently well accepted that tissue macrophages have a more suppressive phenotype, whereas inflammatory macrophages have stimulatory effects. Although there is no established consensus regarding these populations (reviewed [4]), the most widely accepted nomenclature is M1 and M2, or *classically* and *alternatively activated* macrophages, respectively [5,6]. This nomenclature refers to the activation and functional *status* of these cells, and it was first described that M1 are IFN-γ and/or LPS-

* Corresponding author at: Biotechnology Department, IPEN-CNEN, Sao Paulo, Brazil.
E-mail address: mhmarumo@terra.com.br (K. Foguer).

http://dx.doi.org/10.1016/j.biopha.2016.01.035
0753-3322/© 2016 Elsevier Masson SAS. All rights reserved.

stimulated macrophages, whereas M2 macrophages acquire their phenotype upon stimulation with IL-4, IL-10 or TGF-β [5,6]. Due to the opposing nature and function of the aforementioned cytokines, it has also been observed that M1 and M2 macrophages have opposing transcriptional and phenotypic profiles [2,3].

M2 macrophages resemble tissue-resident macrophages that are involved in tissue repair, phagocytosis of cellular debris and immune suppression and have high expression of arginase-1 [7], IL-10 [8] and SOCS-3 [6], to note a few examples. [9] M1 macrophages serve as potent stimulators of the adaptive immune response and express important pro-inflammatory molecules and transcription factors, such as iNOS, IL-12 [9], NF-κB [10] and STAT-1 [11]. Nonetheless, the importance of this cellular population in several physiological as well as pathological processes, such as inflammatory and autoimmune diseases [4,12], pathogenic infections [11] and cancer, has been called into question (reviewed in [13,14]).

It is very well established that the number of tumor infiltrating lymphocytes (TILs) directly correlates with tumor growth, metastasis and patient prognosis [15,16]. Several reports have demonstrated that the infiltration of CD4 or CD8 IFN-γ-secreting lymphocytes results in increased tumor cell death, as well as reduced tumor growth and metastasis, resulting in an improved prognosis and survival rate [15]. This is likely a result of the fact that several important tumor killing mechanisms are triggered by IFN-γ, such as the secretion of NO [17], TNF-α, and increased expression of antigen presenting molecules [4,6].

Unfortunately, tumor cells may develop many different mechanisms to circumvent the immune response, mainly by triggering suppressive mechanisms. For example, some solid tumors may recruit T regulatory cells to the tumors, as well as induce their expansion in draining lymph nodes [18,19]. Interestingly, this is amplified by tolerogenic dendritic cells in the draining lymph nodes, whose increased expression of indoleamine-2,3-dioxigenase (IDO) promotes the differentiation of Tregs [20], rendering the tumors much more refractory to therapeutic intervention [21,22]. This evidence demonstrates the importance of the quality of tumor infiltration by immune cells, i.e., Tregs vs. T effector cells, and also of the interplay between TILs and innate immunity in tumor elimination and patient survival.

TAMs have also gained recent attention, as it has been reported that these cells greatly correlate with tumor progression, metastasis and overall outcome, similar to T cells (reviewed in [14,16]). Indeed, similarly to Tregs, tumor-infiltrating macrophages may actually dampen the immune response in several different ways. For instance, when T cells were transferred to RAG-deficient animals, the presence of Th2 lymphocytes secreting IL-4 and IL-10 greatly reduced the immune effector response, converting TAMs to an M2 phenotype and rendering the animals more susceptible to lung metastasis [23]. Moreover, TAMs are able to secrete significant amounts of the M2 marker CCL2, which in turn may recruit $CD4^+CD25^+Foxp3^+$ Tregs to solid ovarian tumors, promoting their growth and vascularization [24].

Renal cell carcinoma (RCC) is the most common type of kidney cancer and accounts for approximately 3% of human malignancies. [25] In adults, the most common histologic subtype is clear cell RCC (ccRCC). Most patients with ccRCC have a mutation in the tumor suppressor gene von Hippel–Lindau (VHL). The VHL gene encodes the VHL protein, which is capable of down regulating a number of intracellular proteins, including hypoxia inducible factor (HIF). HIF is heterodimeric transcription factor (HIF α/β) that regulates the expression of genes and facilitates the adaptation of tissue during hypoxia. In normoxic conditions, however, VHL protein is involved in the degradation of the HIF α subunit. Loss of function of the VHL gene, even under normal oxygen pressure, results in an increase in HIF and a consequent increase in the transcription of several angiogenic factors such as vascular endothelial growth factor (VEGF), platelet derived growth factor (PDGF) and basic fibroblast growth factor (FbF) [26,27]. The presence of these angiogenic factors justifies the intense vascularization of CCR and contributes substantially to the development and progression of this disease, explaining the high prevalence of metastases (30–40%) in the initial diagnosis of RCC.

Renal cell carcinoma (RCC) is considered to be an immunogenic tumor and is frequently infiltrated by immune cells. However, clinicopathological studies have indicated that patients with higher densities of infiltrating TAMs have significantly poorer relapse-free survival and overall survival rates. Therefore, TAM infiltration appears to be a significant unfavorable prognostic factor in cancer patients and may be a potentially useful prognostic marker of clinical outcomes.

In this work, we evaluated the functional characteristics of TAMs in metastatic lungs of mice that underwent antiangiogenic gene therapy with ES.

2. Material and methods

2.1. Cell Lines

NIH/3T3-LendSN-clone 3 was used for ES expression, and NIH/3T3-LXSN was used as a control, as described in previous work [10]. Both cell lines were maintained in high-glucose (4.5 g/L at 25 mM) DMEM medium (Life Technologies Corporation®, Grand Island, NY, USA) supplemented with 100 U/mL penicillin, 100 μg/mL streptomycin (Gibco® Life Technologies, NY, EUA), and 10% fetal bovine serum (FBS) (Life Technologies Corporation® Grand Island, NY, USA).

The murine kidney carcinoma cell line (Renca), was maintained in RPMI 1640 medium (Life Technologies Corporation® Grand Island, NY, USA) supplemented with 10% fetal bovine serum (Life Technologies Corporation® Grand Island, NY, USA), 2 mM L-glutamine (Gibco® Life Technologies, NY, USA), 1 mM sodium pyruvate (Gibco® Life Technologies, NY, USA), 1% minimal Eagle's medium nonessential amino acids (Gibco® Life Technologies, NY, USA), 100 U/mL penicillin and 100 μg/mL streptomycin (Gibco® Life Technologies, NY, USA).

Both cell lines were maintained at 37 °C in a humidified atmosphere containing 5% CO_2.

2.2. Animals

Male BALB/c mice, aged 8–10 weeks, were obtained from the Animal Facility of IPEN/CNEN-SP, Sao Paulo, Brazil. In these experiments, 24 mice were used (normal group = 8, control group = 8, ES-treated group = 8). All animals were cared for in accordance with the standards of the institute under a protocol approved by the Animal Experimentation Ethics Committee (Number of Process: 0260/12).

2.3. Orthotopic metastatic RCC tumor model

Mice were anesthetized by intraperitoneal injection with ketamine and xylazine (100 mg/kg body weight, Ketalar; Parke-Davis, Morris Plains, NJ, USA and 10 mg/kg body weight, Phoenix Scientific, St. Joseph, MO, USA, respectively). The left flank region was trichotomized and the left kidney was exposed and 2×10^5 Renca cells suspended in 10 μL of Phosphate Buffered Saline (PBS) were injected under the renal capsule with the aid of a glass

syringe (Hamilton®, Reno, NV, USA). The kidney was returned to the posterior region of the abdomen and was sutured at the region of the incision.

7 days after Renca cell inoculation, the kidney was removed by unilateral nephrectomy. Then, mice were divided into two experimental groups: control group and ES-treated group. These groups received a subcutaneous injection of 3.6×10^6 cells NIH/3T3-LXSN or NIH/3T3-LendSN-clone 3, respectively.

2.4. Obtaining plasma from whole blood

At the end of the experiment, which totaled 17 days, mice were euthanized in accordance with current standards of the American Veterinarian Medical Association. Blood samples were collected into test tubes containing heparin. The plasma components were separated from whole blood by centrifugation and then stored in a freezer at −20 °C.

2.5. Determination of plasma ES and cytokine levels

Plasma ES levels were measured using a Mouse Endostatin ELISA Kit (Novateinbio®, Accelerates Research and Development, USA) according to the manufacturer's instructions. The ES concentrations were determined at least in duplicate, and the assay reproducibility was confirmed. ELISA plates were read using the Multiskan EX Microplate Reader (Labsystems, Milford, MA, USA).

The cytokine concentrations were determined using the Milliplex® (Mouse Cytokine Magnetic Bead Panel, Millipore), according to the manufacturer's instructions. The plate was read on Luminex 200™ device and data were processed using the Xponent software. We analyzed data from the mean fluorescence intensity (MFI).

2.6. Isolation of TAMs

The lungs of the mice were perfused with cold saline solution, and after removal they were maintained in pure DMEM medium. The lungs were minced with surgical scissors, treated with an enzyme solution of collagenase D (2.5 mg/mL) (Roche, Mannheim, Germany) diluted in DMEM and incubated at 37 °C for 45 min with continuous agitation. DMEM with 10% FBS was then added, and the samples were centrifuged at 450 × *g* for 5 min at 4 °C. The tissue suspension was passed through a 70-mm cell strainer, subjected to discontinuous Percoll gradient separation (GE Healthcare®, Uppsala, Sweden) using 37 and 70% dilutions, and centrifuged at 950 × *g* for 20 min at 4 °C with the brakes off. The cells were collected from the interface between the different gradients of Percoll and resuspended in the appropriate medium supplemented with 10% FBS. The cells were centrifuged at 450 × *g* at 4 °C for 5 min and resuspended in 1 mL of the appropriate culture medium without serum and counted in a Neubauer chamber.

The isolated cells were seeded in 100-mm cell culture plates in RPMI-1640 medium for 40 min. Non-adherent cells were removed by PBS washes, and adhered cells (TAMs) were used for the following experiments.

2.7. Reverse transcription-polymerase chain reaction (RT-PCR)

RNA was isolated from the adherent cells using the reagent Qiazol (Qiagen, Germantown, MD, USA). cDNA was synthesized from 2 μg total RNA with the first-strand cDNA Synthesis kit (Promega, Heidelberg, Germany), following the manufacturer's instructions. All RT-PCR reactions were performed using the ABsolute Mix SYBR Green qPCR kit (Thermo Scientific® Grand Island, NY, USA). The 20 μL reactions contained 10 μL of 1× SYBR Green qPCR Mix, containing the fluorophore SYBR Green I, Taq polymerase, dNTPs, MgCl2 and buffer the enzyme, and 10 μL containing primers and H_2O. The amplification reaction was performed by the Real Time Step One Plus PCR System (Applied Biosystems®) as follows: 50 °C for 2 minutes, 95 °C for 10 min, and 40 cycles of 95 °C for 15 s and 60 °C for 1 min. The expression levels of target genes calculated using the following equation: relative quantification = $2^{-\Delta\Delta Ct}$. A Ct value was calculated for both the target gene and the reference gene (HPRT) for each sample. This value represents the point at which the amplification signal was detected. From there, the ΔCt was calculated ($Ct_{targetgene} - Ct_{normalizing}$[HPRT]). Subsequently, the ΔΔCt was determined ($\Delta Ct_{sample} - \Delta Ct_{HPRT}$) using normal (healthy lung) tissue to compare the level of target gene expression. The ΔΔCt was used to quantify the relative expression level, where the number 2 is the sum of the primer efficiencies of the target reference genes, where both have 100% efficiency. All primers sequences are shown in Table 1.

2.8. Immunofluorescence

The isolated cells were plated in 24-well plates and after adhesion were fixed in 4% paraformaldehyde at room temperature for 10 min. Then, the cells were washed with PBS and incubated with 1% BSA at 37 °C for 1 h to block nonspecific interactions. Primary antibody to F4/80 (A3-1, MCA497G, AbD Serotec, Kidlington, UK) was incubated at 4 °C overnight. After washes with PBS, the cells were incubated with anti-IgG secondary antibody and conjugated with Alexafluor-645 (Invitrogen, Carlsbad, USA) at room temperature for 1.5 h. Subsequently, the cells were washed with PBS and kept in mounting media (Prolong Gold Antifade Reagent, Invitrogen, Carlsbad, USA) containing 4′,6-diamidino-2-phenylindole (DAPI) in the darkroom at 4 °C until acquisition of images.

2.9. Flow cytometry analysis

Cells were seeded at a density of 1 ×106 per well in a 96-well plate, and incubated with lipopolysaccharide (LPS) (1 μg/mL) (Sigma–Aldrich, St. Louis, MO). Cells were incubated with brefeldin-A (e-Biosciences, San Diego, CA, USA) for 10 h to avoid cytokine secretion, for subsequent intracellular staining. Cells surfaces were then stained with anti-F4/80 antibody conjugated to FITC (BM8, cat. number 11-4801, e-Bioscience, San Diego, CA, USA), anti-CD11c antibody conjugated to PE (N418, cat. number 12-0114, e-Bioscience, San Diego, CA, USA), anti-CD206 antibody conjugated

Table 1
Sequence of Primers used for RT-PCR.

HPRT	Forward (F) 5′-TGGACAGGACTGAAAGACTT-3′
	Reverse (R) 5′-AATGTAATCCAGCAGGTCAG3′
IL-10	Forward (F) 5′-CCTCGTGGAGCCTCAGTTTTC-3′
	Reverse (R) 5′-GAGCACGTCAGGTACATTTCAATT-3′
IL-12	Forward (F) 5′-GCGTGGGAGTGGGATGTG-3′
	Reverse (R) 5′-GCAAAACGATGGCAAACCA-3′
Arg-1	Forward (F) 5′-AACGGGAGGGTAACCATAAGC-3′
	Reverse (R) 5′-GCGCATTCACAGTCACTTAGGT-3′
iNOS	Forward (F) 5′-GGGCAGCCTGTGAGACCTT-3′
	Reverse (R) 5′-TGAAGCGTTTCGGGATCTG-3′
VEGF	Forward (F) 5′-CCAGACCTCTCACCGGAAAG-3′
	Reverse (R) 5′-CTGTCAACGGTGACGATGATG-3′

to AlexaFluor 647 (MR5D3, cat. number MCA2235A647, AbD Serotec, Kidlington, UK), anti-CD80 antibody conjugated to PE (cat. number 12-0801, e-Bioscience, San Diego, CA, USA), anti-CD36 antibody conjugated to PE (cat. number 12-0361, e-Bioscience, San Diego, CA, USA), or anti-CD209 antibody conjugated to PE (cat. number 122091, e-Bioscience, San Diego, CA, USA) and fixed with Cytofix/Cytoperm (BD Biosciences, New Jersey, USA). Cells were then intracellular proteins were stained with anti-IL-10 antibody conjugated to PE (cat number 554467, BD Biosciences, New Jersey, USA), anti-IL-12 antibody conjugated to PE (cat number 554479, BD Biosciences, New Jersey, USA), anti-IL-12 antibody conjugated to PE-Cy7 (cat number 25-7123, e-Bioscience, San Diego, CA, USA) and anti-Arginase I antibody conjugated to PE (cat number IC5868P, BD Biosciences, New Jersey, USA).

Flow cytometry was performed on a FACS Accuri C6 (BD, San Diego, CA) with Csampler software for data analysis.

2.10. Culture of macrophages

Following tissue digestion and isolation of macrophages by density gradient centrifugation, 5×105 macrophages were separated and plated in 96-well plates in RPMI. After 2 h to allow cells to adhere, a wash was performed with PBS, and these cells were stimulated with 1 μg/mL of LPS in RPMI for 48 h. Cell culture supernatant was collected and stored at −20 °C.

2.11. Determination of cytokine levels in the cell culture supernatant

IL-12 and IL-10 levels were analyzed by capture ELISA using kit Mouse IL-12 ELISA Set and mouse IL-10 ELISA Set (BD Biosciences, New Jersey, USA), according to manufacturer's instructions.

2.12. Statistical analysis

Simple comparisons of means were performed by Student's *T* tests. The multiple mean comparisons were performed using one-way or two-way ANOVA followed by Bonferroni's test using the GraphPad Prism program Version 5.0 Windows (GraphPad® Software, San Diego, CA, USA), http://www.graphpad.com. Differences with a p value of $p < 0.05$ were considered statistically significant.

3. Results

ES plasma levels of the normal and experimental groups were measured. The normal group, control group and ES group had plasma levels of 127.1 ± 9.43 μg/mL, 234.02 ± 6.46 μg/mL and 333.9 μg/mL ± 9.21, respectively. The presence of tumor cells led to a 1.84-fold increase in endogenous ES levels in the control group compared with the normal group (normal vs. control $p < 0.001$). The ES group had a 2.62-fold increase in ES plasma levels compared with the normal group (normal vs. ES $p < 0.001$) and a 1.42-fold increase compared with the control group (control vs. ES $p < 0.001$). Circulating ES levels corroborated our previous data [29–36].

3.1. ES treatment decreases anti-inflammatory and pro-angiogenic cytokines

We began our research by measuring the circulating levels of cytokines in all three experimental groups using multiplex cytokine panels. Several cytokines were detected above the lower limits of detection of the assay in the normal group. Interestingly, we did not detect differences in Th1-related cytokines, such as IL-12 and TNF-α in ES-treated animals compared with control animals (Fig. 1A and F). However, ES treatment significantly reduced anti-inflammatory and pro-angiogenic cytokines,

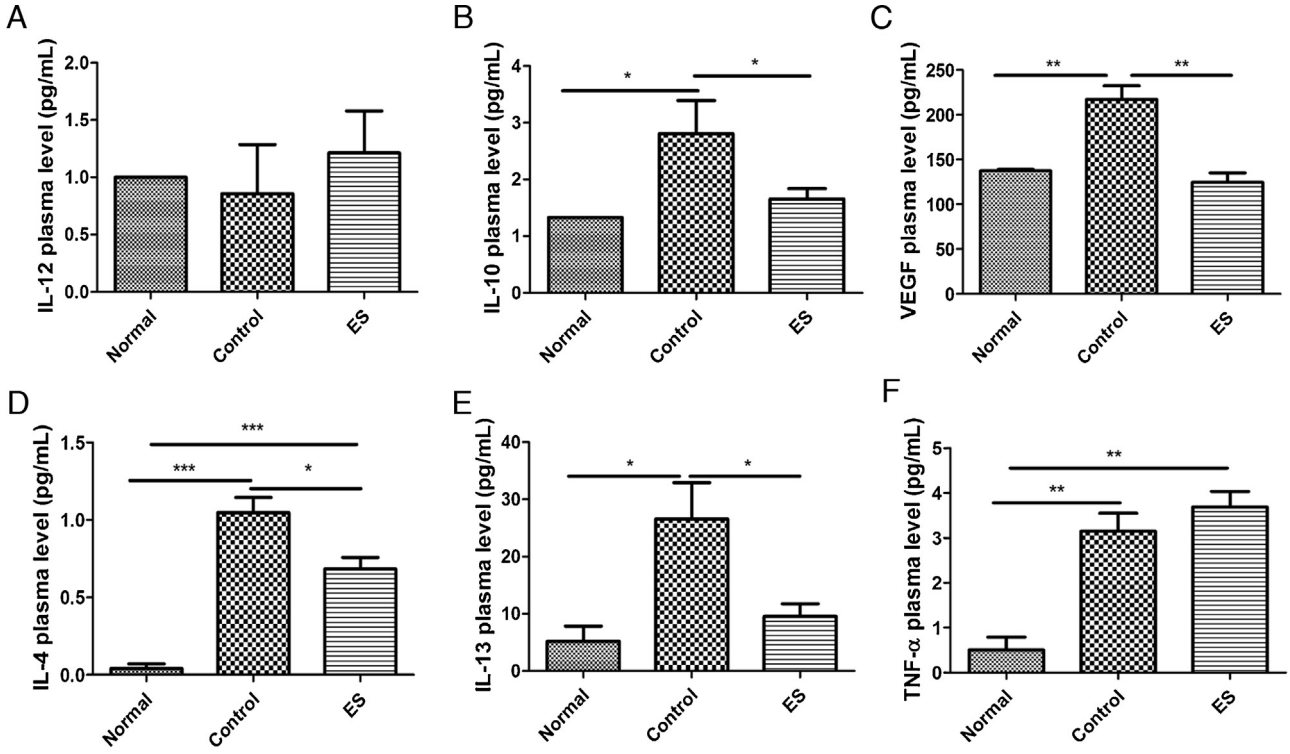

Fig. 1. Determination of plasma levels of IL-12, IL-10, VEGF, IL-4, IL-13 and TNF-α. Circulating levels of pro or anti-inflammatory cytokines were determined in the plasma of control and ES-treated animals according to the materials and methods. $N = 4$. One-way ANOVA followed by Bonferroni by Bonferroni's test. $^{*}p < 0.05$; $^{**}p < 0.01$; $^{***}p < 0.001$.

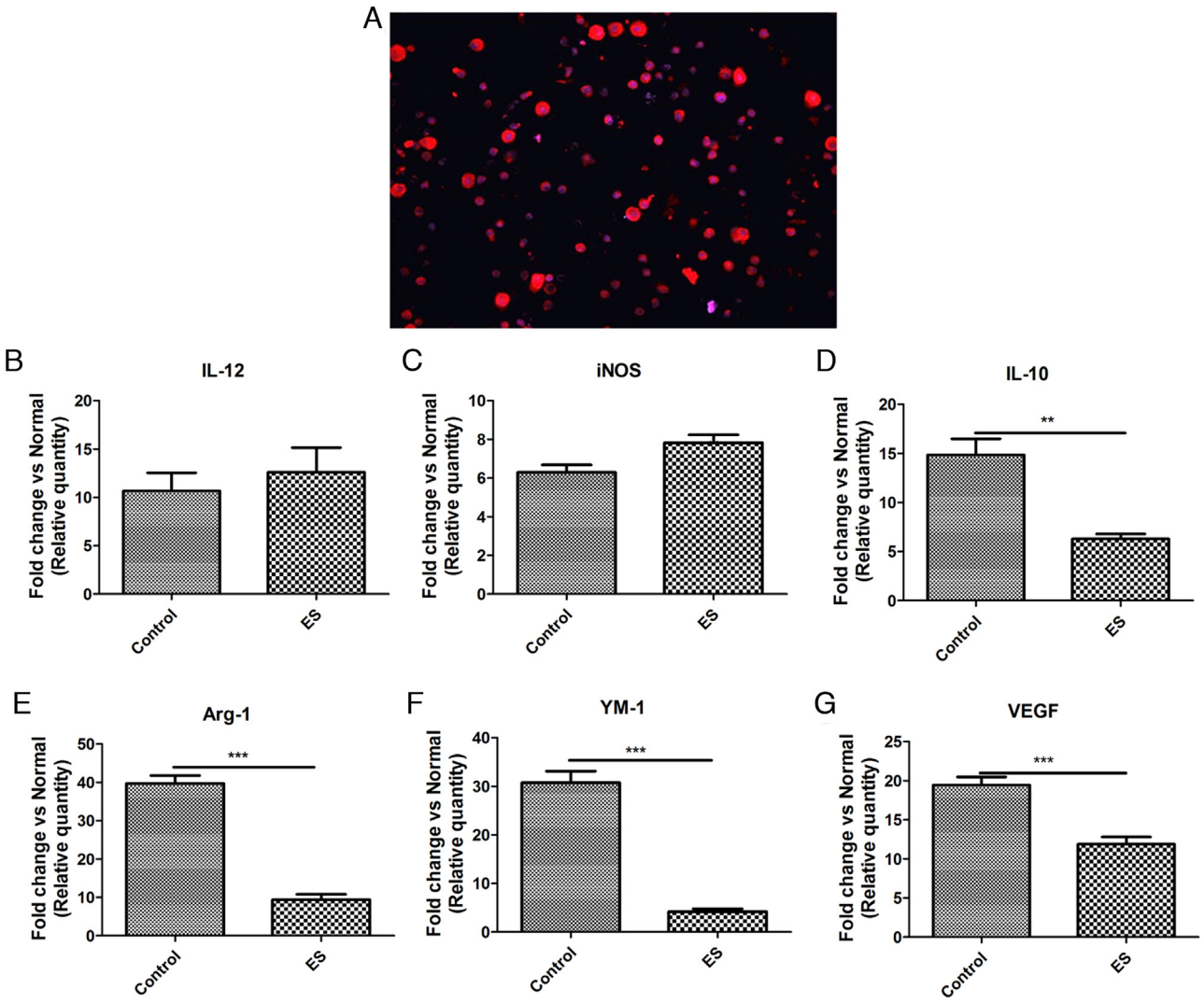

Fig. 2. TAM gene expression profile of M1 and M2 markers. TAMs were obtained, enriched and analyzed according to materials and methods and analyzed for the expression of IL-12, iNOS, IL-10, arginase I, YM-1 and VEGF. (A) Enrichment of TAMs was evaluated by F4/80 (anti-F4/80 Pe) and DAPI (blue) staining. TAMs were visualized at 40× magnification. (B) The gene expression profile was evaluated by qPCR. $N = 4$. Student's t-test $^{**}p < 0.01$; $^{***}p < 0.001$. (For interpretation of the references to color in this figure legend, the reader is referred to the web version of this article.)

including IL4, IL-10, IL-13 and VEGF (Fig. 1B–E), which was expected due to its anti-angiogenic capacity.

3.2. Expression of M2-associated genes were decreased by ES treatment

We next evaluated the gene expression profile of TAMs. Accordingly, TAMs were isolated from metastatic lungs and plated to enrich the macrophages by adherence. The lung weight of the samples ranged from 0.1 g to 0.5 g and the number of TAMs collected ranged from 1.0 × 106 to 2.0 × 106 cells. F4/80 labeling confirmed the enrichment of the isolated macrophages of the lungs (Fig. 2A). RNA was isolated from the macrophages to carry out gene expression analysis.

The gene expression of the classic M1 markers IL-12, iNOS did not change significantly in response to ES treatment (Fig. 2B and C). Interestingly, ES treatment significantly reduced the expression of several M2 markers, such as IL-10, Arg-1, VEGF and a novel phenotype marker, YM-1 (Fig. 2D–G).

3.3. Macrophage recruitment in metastatic lungs was not altered by ES treatment

To corroborate previous findings, we next evaluated the frequency of M1 and M2 macrophages among the TAMs by flow cytometry. Initially, analysis of the side scatter profile beam (SSC) and forward scatter profile (FSC) was performed for *gating*. As shown in Fig. 3A, TAMs accounted for approximately 51.2% of the total population (Fig. 3A). This population was then analyzed for the expression of F4/80 (Fig. 3B). There was a significant increase in the population of F4/80$^+$ TAMs in the control group compared with the normal group (17.26 ± 5.98 vs. 12.01 ± 0.46 F4/80$^+$ %, $p < 0.05$) (Fig. 3C). No changes were observed among the other groups.

3.4. ES therapy decreases M2 macrophages in the tumor microenvironment

Next, TAMs were quantified according to M1 and M2 phenotypes. F4/80$^+$/CD11c$^+$ and F4/80$^+$/CD80$^+$ populations

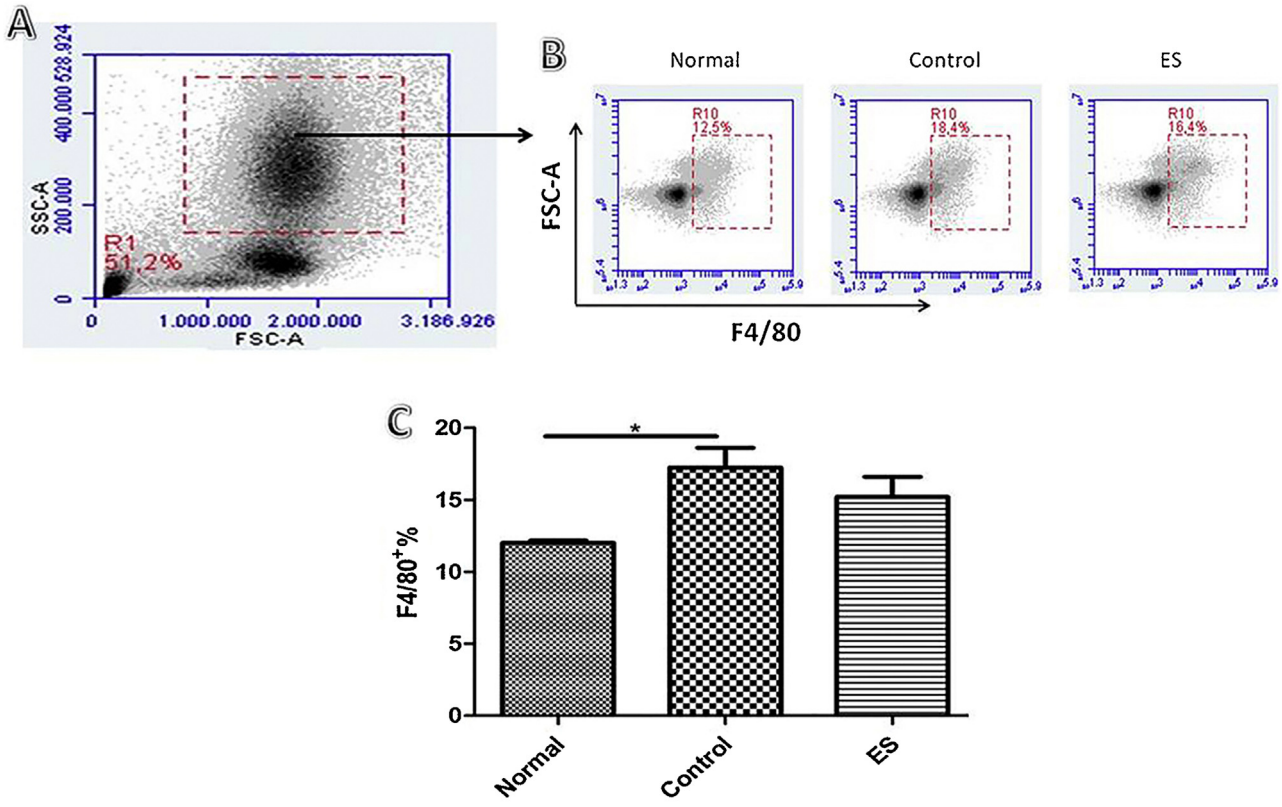

Fig. 3. Assessment of the frequency of TAMs in the lungs of mice by flow cytometry. (A) Representative gate showing macrophage gating strategy. (B) Representative scatter charts show the respective percentage of F4/80$^+$ cells, which are quantified, in representative graphs (C). $^*p < 0.05$. $N = 4$. One-way ANOVA followed by Bonferroni's test.

increased significantly in the metastatic lungs of control group mice (Fig. 4A–D). However, ES treatment caused no change in the frequency of these populations. Similarly, M2 markers (CD206, CD209, CD36 and arginase 1) were significantly increased in the lungs of control group mice. However, ES treatment significantly decreased the number of M2-polarized macrophages. (Fig. 4E–L).

The production of pro- and anti-inflammatory cytokines was measured in the macrophages. F4/80/CD11c and F4/80/CD80 cells were selected (Fig. 4A and C), and IL-12 was identified from them.

The presence of lung metastases resulted in a significant increase in F4/80$^+$/CD11c$^+$/IL-12$^+$ and F4/80$^+$/CD80$^+$/IL-12$^+$ cells. However, treatment with ES did not cause a significant change in any of these populations (Fig. 5A–D). The control group mice had significantly elevated levels of IL-10-producing macrophages (F4/80$^+$/CD206$^+$/IL-10$^+$, F4/80$^+$/CD209$^+$/IL-10$^+$ and F4/80$^+$/CD36$^+$/IL-10$^+$) compared with the normal mice. Treatment with ES promoted a significant reduction in these populations (Fig. 5E–I).

3.5. Determination of cytokine levels in the cell culture supernatant

The determination of IL-12 and IL-10 in the supernatants of the macrophage cultures was performed after stimulation with LPS. IL-12 levels were not significantly different between groups (normal *vs.* control, $p = 0.45$; normal vs. ES, $p = 0.07$; and control *vs.* ES, $p = 0.45$). However, the amount of IL-10 present in the culture supernatants was significant increased in the control group compared with the normal ($p < 0.05$) and ES ($p < 0.01$) groups (Fig. 6).

4. Discussion

In the present work, we sought to evaluate whether treatment with recombinant ES would modulate the profile of TAMs in our model of lung metastasis. ES is a 20-kDa fragment resulting from cleavage of the collagen XVIII COOH terminus. This portion has been described to inhibit endothelial cell proliferation, migration and invasion, and to dramatically reduce tumor growth and metastasis in several mouse models with no serious side effects [28–36]. Of note, using the same model, we have previously published that ES treatment increased the frequency of pro-inflammatory TILs, mainly IFN-γ-secreting CD4, CD8 and NK cells, resulting in a reduced number of lung tumor nodules, reduced metastasis and a higher survival rate [17]. Thus, besides its anti-angiogenic activity, we have previously demonstrated that ES also displays an important stimulatory function on T lymphocytes. Here, our approach was to evaluate whether this effect could be extended, either directly or indirectly, to TAMs.

Our results clearly demonstrate a contraction of the regulatory M2 macrophages within the tumoral lung nodules; however, we observed no change in pro-inflammatory M1 macrophages. We observed a decrease in several important M2 markers in vivo, such as arginase-1, Ym-1 and VEGF. Previous research has shown that reduced intra-tumoral O_2 tension induces high expression of HIF-1α that specifically up-regulates suppressive and pro-angiogenic molecules, such as PD-1 and VEGF [37]. The importance of VEGF in tumor growth and establishment of metastases is worth noting. Accordingly, we observed that ES treatment not only reduced the expression of VEGFR in macrophages isolated from the metastatic nodules but also that the ES-treated animals had less soluble VEGF in plasma than the control group.

Associated with these findings, we also demonstrated through flow cytometry and intracellular staining that there is not only a reduction of M2 F4/80$^+$CD36$^+$CD206$^+$CD209$^+$ macrophages but also a reduction in IL-10 secretion by these populations. The quantification of the cytokines in culture supernatant also revealed reduced levels of secreted IL-10 in the ES-treated group. IL-10 is

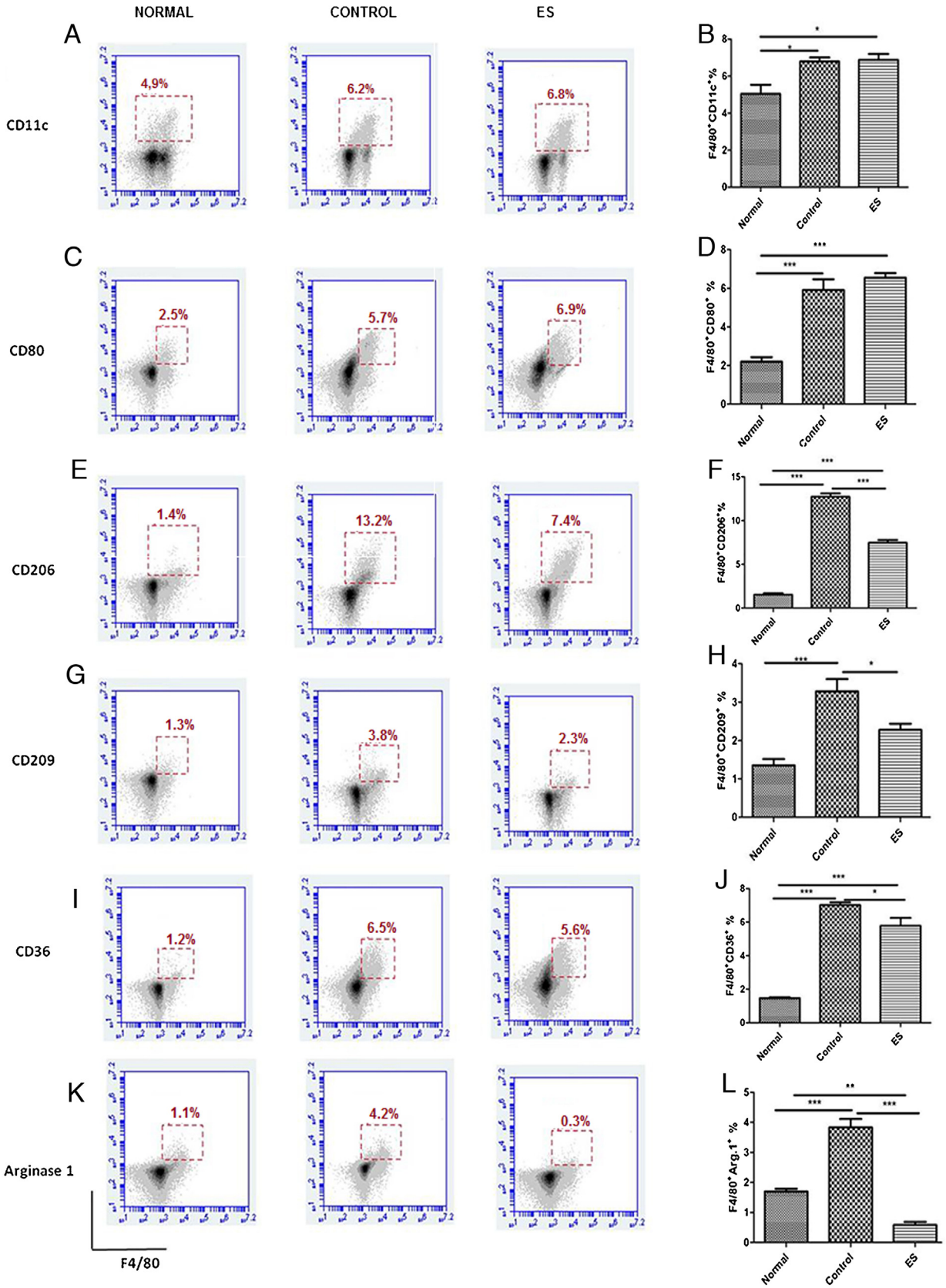

Fig. 4. Assessment of M1 and M2 macrophage subsets among TAMs by flow cytometry. (A, C, E, G, I, K) Representative scatter charts show the percentage of F4/80$^+$CD11$^+$, F4/80$^+$CD80$^+$, F4/80$^+$CD206$^+$, F4/80$^+$CD209$^+$, F4/80$^+$ CD36$^+$, and F4/80$^+$Arg1$^+$cells. (B, D, F, H, J, L) Statistical analysis for the data represented in each panel was performed using a one-way ANOVA followed by a Bonferroni's test. N = 4. $^*p < 0.05$, $^{**}p < 0.01$, $^{***}p < 0.001$.

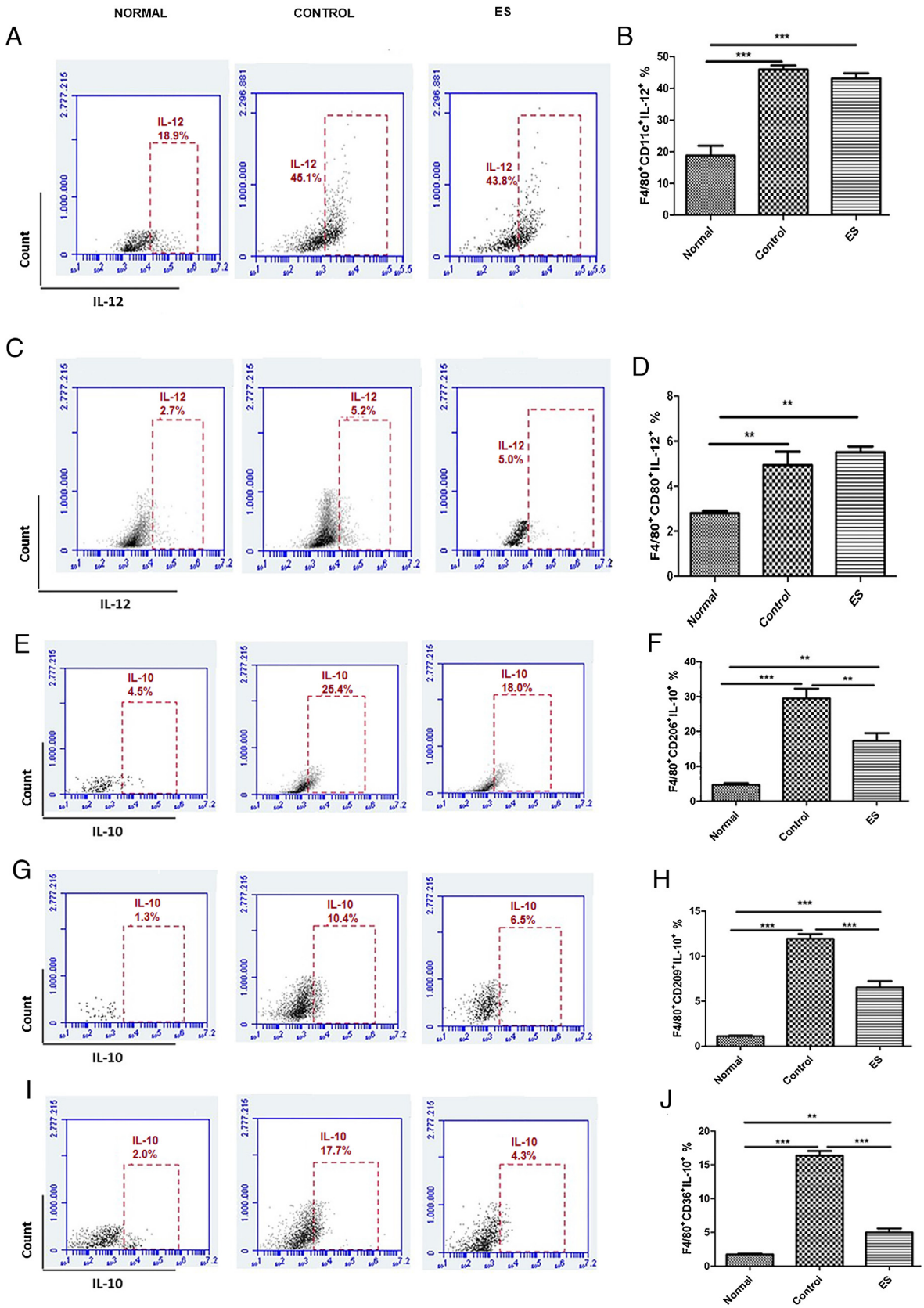

Fig. 5. Assessment of IL-10- and IL-12-producing macrophages in the lungs of normal, control and ES-treated mice by flow cytometry. (A and C) Representative scatter charts show the percentages of $F4/80^+/CD11c^+/IL\text{-}12^+$ and $F4/80^+/CD80^+/IL\text{-}12^+$ cells. (B) (E, G, I) Representative scatter charts show the percentages of $F4/80^+/CD206^+/IL\text{-}10^+$, $F4/80^+/CD209^+/IL\text{-}10^+$ and $F4/80^+/CD36^+/IL\text{-}10^+$ cells. (B, D, F, H, J) Statistical analysis for the data represented in each panel was performed using one-way ANOVA followed by Bonferroni's test. $N = 4$. $^{*}p < 0.05$, $^{**}p < 0.01$, $^{***}p < 0.001$.

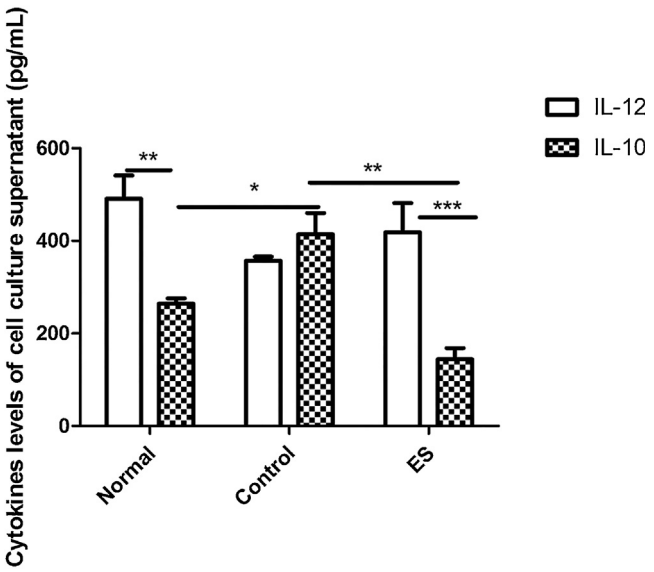

Fig. 6. Determination of IL-12 and IL-10 levels in the macrophage cell culture supernatant. No significant difference in IL-12 production was found between groups (normal vs. control, $p = 0.45$, normal vs. ES, $p = 0.07$ and control vs. ES, $p = 0.45$). A significant increase in the level of secreted IL-10 was observed in the control group compared with the normal group ($^{*}p < 0.05$) and ES ($^{**}p < 0.01$). Secretion of IL-12 was significantly higher than IL10 in the normal and ES groups ($^{*}p < 0.01$ and $^{***}p < 0.001$, respectively). $N = 4$ one-way ANOVA followed by Bonferroni's test.

one of the most important suppressive cytokines that directly correlates with immunosuppression and tumor aggressiveness, as shown in breast tumors [38] and HPV-related cancer [39,40]. These findings may indicate that the changes observed for TILs described in our previous research (i.e., the increase in IFN-γ-secreting T and NK cells) may be responsible for these changes observed. Furthermore, we may not exclude the possibility that ES acts directly on macrophages or even in a more systemic way, as it has recently been described as a androgen receptor antagonist [41]. The reduction in IL-10 is coincident with reduction of IL-4, which is also important in skewing macrophages toward the M2 phenotype. It is worth mentioning, however, that although these suppressive cytokines were reduced, no changes were observed for IL-12 and IL-1β secretion, leading us to speculate that ES may be more effective in abrogating or dampening M2 expansion, rather than promoting M1 differentiation.

5. Conclusion

In summary, our research corroborates previous observations that ES has important anti-tumoral activity. However, aside from promoting an effective T cell response and interferon-γ secretion, we show here that this switch is extended to TAMs, complicating the maintenance of pro-tumorigenic M2 macrophages and thus favoring tumor elimination. Although we refer to tumor infiltrating immune cells as an "*inflammatory infiltrate*", many of these cells in fact display more of a suppressive phenotype rather than an anti-tumoral profile. Our findings highlight the conundrum that is the anti-tumor immune response and the pleiotropic effect of ES in this model.

Conflict of interest

The authors declare that they have no conflicts of interest concerning this article.

Acknowledgements

We would like to thank Ms. Evelin Caroline da Silva for their valuable technical support on this project. This study was supported by FAPESP (Process number: 2011/18703-2) CNPq (Process number: 473102/2012-9) and CAPES/PNPD.

References

[1] T.A. Wynn, A. Chawla, J.W. Pollard, Macrophage biology in development, homeostasis and disease, Nature 496 (2013) 445–455, doi:http://dx.doi.org/10.1038/nature12034.
[2] E.L. Gautier, T. Shay, J. Miller, M. Greter, C. Jakubzick, S. Ivanov, et al., Gene-expression profiles and transcriptional regulatory pathways that underlie the identity and diversity of mouse tissue macrophages, Nat. Immunol. 13 (2012) 1118–1128, doi:http://dx.doi.org/10.1038/ni.2419.
[3] A.D.A. Cassado, M.R. D'Império Lima, K.R. Bortoluci, Revisiting mouse peritoneal macrophages: heterogeneity, development, and function, front, Immunology 6 (2015) 1–9, doi:http://dx.doi.org/10.3389/fimmu.2015.00225.
[4] F.O. Martinez, S. Gordon, The M1 and M2 paradigm of macrophage activation: time for reassessment, F1000Prime Rep. 6 (2014) 1–13, doi:http://dx.doi.org/10.12703/P6-13.
[5] J.P. Edwards, X. Zhang, K.A. Frauwirth, D.M. Mosser, Biochemical and functional characterization of three activated macrophage populations, Cytokines 80 (2006) 1298–1307, doi:http://dx.doi.org/10.1189/jlb.0406249.1.
[6] P.J. Murray, J.E. Allen, S.K. Biswas, E.A. Fisher, D.W. Gilroy, S. Goerdt, et al., Macrophage activation and polarization: nomenclature and experimental guidelines, Immunity 41 (2014) 14–20, doi:http://dx.doi.org/10.1016/j.immuni.2014.06.008.
[7] K.C. El Kasmi, J.E. Qualls, J.T. Pesce, A.M. Smith, R.W. Thompson, M. Henao-Tamayo, et al., Toll-like receptor-induced arginase 1 in macrophages thwarts effective immunity against intracellular pathogens, Nat. Immunol. 9 (2008) 1399–1406, doi:http://dx.doi.org/10.1038/ni.1671.
[8] K.K. Wijesundera, T. Izawa, A.H. Tennakoon, H.M. Golbar, M. Tanaka, M. Kuwamura, et al., M1-/M2-macrophages contribute to the development of GST-P-positive preneoplastic lesions in chemically-induced rat cirrhosis, Exp. Toxicol. Pathol. 67 (2015) 467–475, doi:http://dx.doi.org/10.1016/j.etp.2015.05.002.
[9] W.T. Festuccia, P. Pouliot, I. Bakan, D.M. Sabatini, M. Laplante, Myeloid-specific rictor deletion induces M1 macrophage polarization and potentiates in vivo pro-inflammatory response to lipopolysaccharide, PLoS One 9 (2014) e95432, doi:http://dx.doi.org/10.1371/journal.pone.0095432.
[10] H. Dai, D. Xu, J. Su, J. Jang, Y. Chen, Transmembrane protein 106a activates mouse peritoneal macrophages via the MAPK and NF-κB signaling pathways, Sci. Rep. 5 (2015) 12461, doi:http://dx.doi.org/10.1038/srep12461.
[11] L.R. Filgueiras, S.L. Brandt, S. Wang, Z. Wang, D.L. Morris, C. Evans-molina, et al., Leukotriene B4—mediated sterile inflammation promotes susceptibility to sepsis in a mouse model of type 1 diabetes, Sci. Signal. 8 (2015) 1–10, doi:http://dx.doi.org/10.1126/scisignal.2005568.
[12] M.S. Weber, T. Prod'homme, S. Youssef, S.E. Dunn, C.D. Rundle, L. Lee, et al., Type II monocytes modulate T cell-mediated central nervous system autoimmune disease, Nat. Med. 13 (2007) 935–943, doi:http://dx.doi.org/10.1038/nm1620.
[13] D. Nagorsen, S. Voigt, E. Berg, H. Stein, E. Thiel, C. Loddenkemper, Tumor-infiltrating macrophages and dendritic cells in human colorectal cancer: relation to local regulatory T cells, systemic T-cell response against tumor-associated antigens and survival, J.Transl. Med. 5 (2007) 1–8, doi:http://dx.doi.org/10.1186/1479-5876-5-62.
[14] B.Z. Qian, J.W. Pollard, Macrophage diversity enhances tumor progression and metastasis, Cell 141 (2010) 39–51, doi:http://dx.doi.org/10.1016/j.cell.2010.03.014.
[15] F.G. Rocha, F.B. Calvo, K.C. Chaves, J.P. Peron, R.F. Marques, T.R. de Borba, et al., Endostatin- and interleukin-2-expressing retroviral bicistronic vector for gene therapy of metastatic renal cell carcinoma, J. Gene Med. (2011) 148–157, doi:http://dx.doi.org/10.1002/jgm.
[16] C. Reissfelder, S. Stamova, C. Gossmann, M. Braun, A. Bonertz, U. Walliczek, et al., Tumor-specific cytotoxic T lymphocyte activity determines colorectal cancer patient prognosis, J. Clin. Invest. 125 (2015) 1–13, doi:http://dx.doi.org/10.1172/JCI74894.an.
[17] F.G.D.G. Rocha, K.C.B. Chaves, R. Chammas, J.P.S. Peron, L.V. Rizzo, N. Schor, et al., Endostatin gene therapy enhances the efficacy of IL-2 in suppressing metastatic renal cell carcinoma in mice, Cancer Immunol. Immunother. 59 (2010) 1357–1365, doi:http://dx.doi.org/10.1007/s00262-010-0865-6.
[18] F.R.F. Nascimento, E.A. Gomes, M. Russo, A.P. Lepique, Interferon regulatory factor (IRF)-1 is a master regulator of the cross talk between macrophages and L929 fibrosarcoma cells for nitric oxide dependent tumoricidal activity, PLoS One 10 (2015) e0117782, doi:http://dx.doi.org/10.1371/journal.pone.0117782.
[19] J.S. Tzartos, M.A. Friese, M.J. Craner, J. Palace, J. Newcombe, M.M. Esiri, et al., Interleukin-17 production in central nervous system-infiltrating T cells and glial cells is associated with active disease in multiple sclerosis, Am. J. Pathol. 172 (2008) 146–155, doi:http://dx.doi.org/10.2353/ajpath.2008.070690.
[20] Y. Shigematsu, T. Hanagiri, H. Shiota, K. Kuroda, T. Baba, Y. Ichiki, et al., Immunosuppressive effect of regulatory T lymphocytes in lung cancer, with

special reference to their effects on the induction of autologous tumor-specific cytotoxic T lymphocytes, Oncol. Lett. 4 (2012) 625–630, doi:http://dx.doi.org/10.3892/ol.2012.815.
[21] M. Brenk, M. Scheler, S. Koch, J. Neumann, O. Takikawa, G. Häcker, et al., Tryptophan deprivation induces inhibitory receptors ILT3 and ILT4 on dendritic cells favoring the induction of human $CD4^+$ $CD25^+$ $Foxp3^+$ T regulatory cells, J. Immunol. 183 (2009) 145–154, doi:http://dx.doi.org/10.4049/jimmunol.0803277.
[22] R.B. Holmgaard, D. Zamarin, D.H. Munn, J.D. Wolchok, J.P. Allison, Indoleamine 2,3-dioxygenase is a critical resistance mechanism in antitumor T cell immunotherapy targeting CTLA-4, J. Exp. Med. 210 (2013) 1389–1402, doi:http://dx.doi.org/10.1084/jem.20130066.
[23] S. Maleki Vareki, M. Rytelewski, R. Figueredo, D. Chen, P.J. Ferguson, M. Vincent, et al., Indoleamine 2,3-dioxygenase mediates immune-independent human tumor cell resistance to olaparib, gamma radiation, and cisplatin, Oncotarget 5 (2014) 2778–2791.
[24] D.G. DeNardo, J.B. Barreto, P. Andreu, L. Vasquez, D. Tawfik, N. Kolhatkar, et al., CD4+ T cells regulate pulmonary metastasis of mammary carcinomas by enhancing protumor properties of macrophages, Cancer Cell 16 (2009) 91–102, doi:http://dx.doi.org/10.1016/j.ccr.2009.06.018.
[25] T.J. Curiel, G. Coukos, L. Zou, X. Alvarez, P. Cheng, P. Mottram, et al., Specific recruitment of regulatory T cells in ovarian carcinoma fosters immune privilege and predicts reduced survival, Nat. Med. 10 (2004) 942–949, doi:http://dx.doi.org/10.1038/nm1093.
[26] B.L. Steffen Weikert, Contemporary epidemiology of renal cell carcinoma: perspectives of primary prevention, World J. Urol. 28 (2010) 247–252.
[27] A.C. Nardi, S.D.C. Zequi, O.A.C. Clark, J.C. Almeida, S. Glina, Epidemiologic characteristics of renal cell carcinoma in Brazil, Int. Braz. J. Urol. 36 (2010) 151–157, doi:http://dx.doi.org/10.1590/S1677-55382010000200004.
[28] E.L. Coutinho, L.N.D.S. Andrade, R. Chammas, L. Morganti, N. Schor, M.H. Bellini, Anti-tumor effect of endostatin mediated by retroviral gene transfer in mice bearing renal cell carcinoma, FASEB J. 21 (2007) 3153–3161, doi:http://dx.doi.org/10.1096/fj.07-8412com.
[29] F.G. De Góes Rocha, K.C.B. Chaves, C.Z. Gomes, C.B. Campanharo, L.C. Courrol, N. Schor, et al., Erythrocyte protoporphyrin fluorescence as a biomarker for monitoring antiangiogenic cancer therapy, J. Fluoresc. 20 (2010) 1225–1231, doi:http://dx.doi.org/10.1007/s10895-010-0672-7.
[30] K.C.B. Chaves, J.P.S. Peron, R. Chammas, L.T. Turaça, J.B. Pesquero, M.S. Braga, et al., Endostatin gene therapy stimulates upregulation of ICAM-1 and VCAM-1 in a metastatic renal cell carcinoma model, Cancer Gene Ther. 19 (2012) 558–565, doi:http://dx.doi.org/10.1038/cgt.2012.32.
[31] K.C.B. Chaves, L.T. Turaça, J.B. Pesquero, G. Mennecier, M.L.Z. Dagli, R. Chammas, et al., Fibronectin expression is decreased in metastatic renal cell carcinoma following endostatin gene therapy, Biomed. Pharmacother. 66 (2012) 464–468, doi:http://dx.doi.org/10.1016/j.biopha.2012.04.003.
[32] M.D.S. Braga, K.B. Chaves, R. Chammas, N. Schor, M.H. Bellini, Endostatin neoadjuvant gene therapy extends survival in an orthotopic metastatic mouse model of renal cell carcinoma, Biomed. Pharmacother. 66 (2012) 237–241, doi:http://dx.doi.org/10.1016/j.biopha.2011.11.002.
[33] M.S. Braga, T.L. Turaça, K. Foguer, K.C.B. Chaves, J.B. Pesquero, R. Chammas, et al., Vascular endothelial growth factor as a biomarker for endostatin gene therapy, Biomed. Pharmacother. 67 (2013) 511–515, doi:http://dx.doi.org/10.1016/j.biopha.2013.04.008.
[34] M.S. Braga, K. Foguer, K.C. Barbosa Chaves, L. de Sá Lima, C. Scavone, M.H. Bellini, Involvement of the NF-κB/p50/Bcl-3 complex in response to antiangiogenic therapy in a mouse model of metastatic renal cell carcinoma, Biomed. Pharmacother. (2014), doi:http://dx.doi.org/10.1016/j.biopha.2014.07.008.
[35] M.S. O'Reilly, T. Boehm, Y. Shing, N. Fukai, G. Vasios, W.S. Lane, et al., Endostatin: an endogenous inhibitor of angiogenesis and tumor growth, Cell 88 (1997) 277–285, doi:http://dx.doi.org/10.1016/S0092-8674(00) 81848-6.
[36] J.G. Pan, X. Zhou, G.W. Zeng, R.F. Han, Suppression of bladder cancer growth in mice by adeno-associated virus vector-mediated endostatin expression, Tumor Biol. 32 (2011) 301–310, doi:http://dx.doi.org/10.1007/s13277-010-0122-9.
[37] A.L. Doedens, C. Stockmann, M.P. Rubinstein, D. Liao, N. Zhang, D.G. DeNardo, et al., Macrophage expression of hypoxia-inducible factor-1 alpha suppresses T-cell function and promotes tumor progression, Cancer Res. 70 (2010) 7465–7475, doi:http://dx.doi.org/10.1158/0008-5472.CAN-10-1439.
[38] T.S. Sousa, R. Brion, M. Lintunen, P. Kronqvist, J. Sandholm, J. Mönkkönen, et al., Human breast cancer cells educate macrophages toward the M2 activation status, Breast Cancer Res. 17 (2015) 101, doi:http://dx.doi.org/10.1186/s13058-015-0621-0.
[39] T.T.M. Prata, C.M. Bonin, A.M.T. Ferreira, C.T.J. Padovani, C.E.D.S. Fernandes, A.P. Machado, et al., Local immunosuppression induced by high viral load of human papillomavirus: characterization of cellular phenotypes producing interleukin-10 in cervical neoplastic lesions, Immunology (2015) 113–121, doi:http://dx.doi.org/10.1111/imm.12487.
[40] Y.-H. Ahn, S.-O. Hong, J.H. Kim, K.H. Noh, K.-H. Song, Y.-H. Lee, et al., The siRNA cocktail targeting interleukin 10 receptor and transforming growth factor-β receptor on dendritic cells potentiates tumour antigen-specific $CD8^+$ T cell immunity, Clin. Exp. Immunol. 181 (2015) 164–178, doi:http://dx.doi.org/10.1111/cei.12620.
[41] J.H. Lee, T. Isayeva, M.R. Larson, A. Sawant, H.-R. Cha, D. Chanda, et al., Endostatin: a novel inhibitor of androgen receptor function in prostate cancer, Proc. Natl. Acad. Sci. 112 (2015) 1392–1397, doi:http://dx.doi.org/10.1073/pnas.1417660112.